ChemComm

Accepted Manuscript

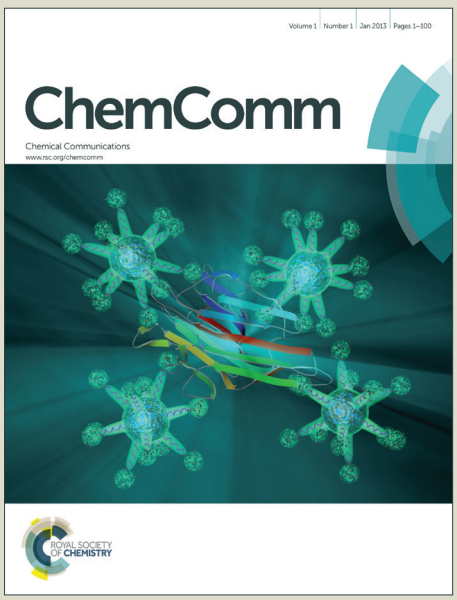

ROYAL SOCIETY OF CHEMISTRY

www.rsc.org/chemcomm

Cite this: DOI: 10.1039/c0xx00000x

www.rsc.org/xxxxxx

ARTICLE TYPE

Fluorescent Bilayer Nanocoils from an Asymmetric Perylene Diimide with Ultrasensitivity for Amine Vapors

Yue E,[a, b‡] Xiaojie Ma,[b‡] Yifan Zhang,[b] Yibin Zhang,[b] Ran Duan,[b] Hongwei Ji,[b] Jing Li,*[a] Yanke Che,*[b] Jincai Zhao[b]

Received (in XXX, XXX) Xth XXXXXXXXX 20XX, Accepted Xth XXXXXXXXX 20XX
DOI: 10.1039/b000000x

Highly fluorescent bilayer nanocoils assembled from an asymmetric perylene diimide exhibit unprecedented sensitivity to trace amines, that is, three orders of magnitude greater than our previously reported solid nanofibers. The coiled nanostructure design for new sensing materials offers a novel option for optimizing the sensitivities of fluorescence sensors based on organic nanomaterials.

Fluorescence sensors based on organic materials are a simple and rapid approach to the optical detection of a specific analyte vapor.[1-3] To maximize the performance of these sensors, a high fluorescence quantum yield and a high porosity should be achieved simultaneously.[3] Nevertheless, simultaneously obtaining these properties remains a significant challenge. In particular, the currently available n-type organic materials are considerably limited compared to the more common p-type materials.[4,5] Perylene diimide (PDI) represents a unique class of n-type semiconductor, and it has been fabricated into various one-dimensional (1D) nanostructures, such as nanoribbons and nanofibers,[2,6-10] and has been widely used in optoelectronics.[2,8,11,12] Although a few nanofibers or gels composed of core-substituted PDI derivatives have been reported to exhibit high fluorescence,[9,13,14] the construction of highly fluorescent porous nanocoils from either core-substituted or core-unsubstituted PDI molecules has not yet been achieved.

We recently observed that nanofibers with interior nanopores formed from p-type organic semiconductors exhibited greatly enhanced fluorescence sensitivity toward explosive analytes (e.g., trinitrotoluene, TNT) compared to solid nanofibers.[15] This observation motivated us to construct nanostructures with interior pores from n-type PDI molecules and to explore their sensitivity for the fluorescent detection of trace amines. In this work, we report the successful fabrication of highly fluorescent bilayer nanocoils (with a fluorescence quantum yield of 25%, as determined using the integrating sphere method) through the self-assembly of an elaborately designed asymmetric perylene diimide, **1** (Figure 1a). A comparison of the nanostructures created from other asymmetric PDI molecules (Figure 1a) suggests that a subtle choice of the polar side chain creates a balanced interplay among molecular steric hindrance, π-interactions, and hydrophobic interactions, thereby resulting in the formation of the fluorescent coiled nanostructure. After being deposited onto a substrate, these fluorescent bilayer nanocoils with interior porosity exhibit unprecedented ultrasensitivity to vapor-phase amines, even exhibiting sensitivities that are enhanced by three orders of magnitude compared to those of solid nanofibers that we previously reported.[6,16]

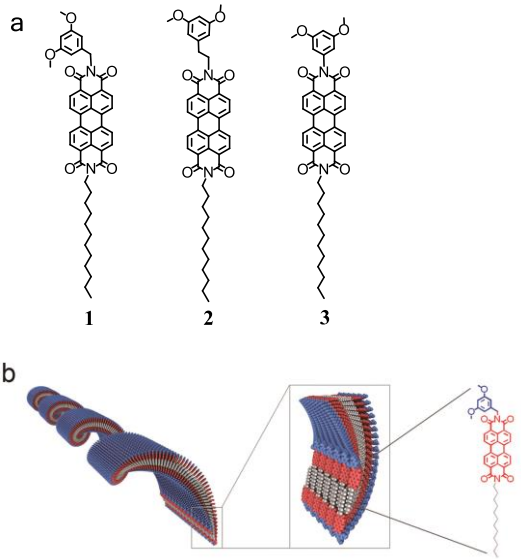

Figure 1 (a) Molecular structures of compounds **1-3**. (b) Schematic representation of the self-assembly of molecule **1** into nanocoils.

The detailed synthesis of compound **1**, which bears polar 3,5-dimethoxybenzyl as one side chain and dodecyl as the other side chain (Figure 1a), is described in the Supporting Information. The self-assembly of the molecule into well-defined nanostructures was achieved through the injection of 0.3 mL of a chloroform solution of **1** (0.14 mM) into 5 mL of ethanol followed by aging for 3 days. Transmission electron microscopy (TEM) and scanning electron microscopy (SEM) images clearly revealed the formation of a helical nanostructure (i.e., nanocoil) from **1** (Figures 2a and 2b). Closer examination of a magnified TEM image revealed that the nanocoil has a diameter of 20 nm and a pitch length of ca. 35 nm (Figure 2c). The wall thickness of the nanocoil was also determined to be ca. 5 nm (Figure 2c), which corresponds to the length of a bilayer structure composed of molecules of **1**. Considering the polarity of the 3,5-dimethoxybenzyl side chains, the bilayer structure of **1** formed in ethanol should be interdigitated

by long alkyl chains, concomitantly having the polar 3,5-dimethoxybenzyl side chains cover the surface. X-ray diffraction (XRD) measurements (see Figure S1 in the supporting information) revealed a dominant diffraction peak at 2.1 nm, which was assigned to the interlayer distance and was consistent with the half of the aforementioned wall thickness determined from the TEM image (Figure 2c). Furthermore, d-spacings of 0.81 nm and 0.47 nm, assigned to the distance between the π-stacks and the center-to-center distance between the π-stacked molecules of **1**, were also observed. Such a nanocoil structure is reminiscent of other helical systems formed from various amphiphilic molecules.[17-21] Note that these nanocoils were thermodynamically stable in ethanol at room temperature and that they still retained the same morphology and optical properties even after being suspended in ethanol for months. This behavior is in sharp contrast to that of kinetically favored nanocoils.[17,20,21]

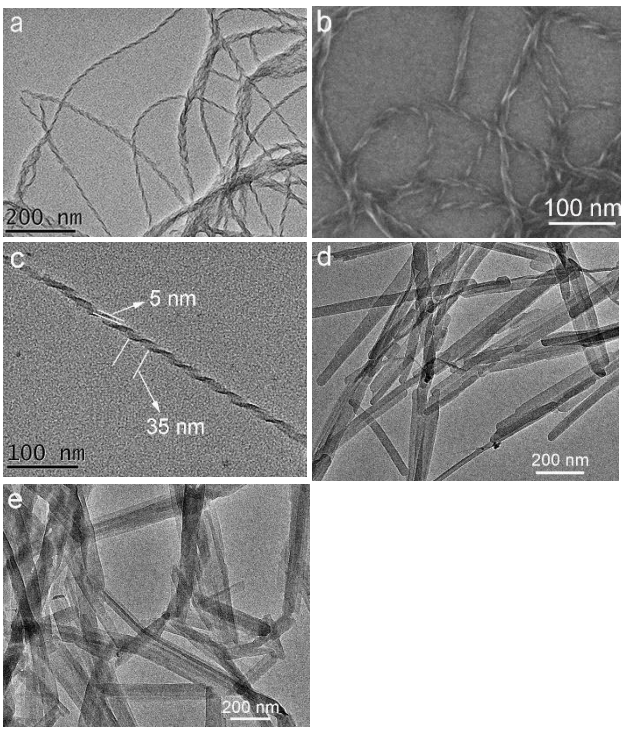

Figure 2 TEM image of the nanocoils formed from **1**. (b) SEM image of the nanocoils formed from **1** deposited onto a silica substrate. (c) TEM image of a single nanocoil formed from **1**. (d) TEM image of the nanoribbons formed from **2**. (e) TEM image of the nanoribbons formed from **3**.

The coiled nanostructure likely forms because the 3,5-dimethoxyphenyl group attached by the methylene linker results in a certain tilting angle relative to the planar PDI backbone that forces the PDI molecules to adopt a helical π-stacking geometry to release steric hindrance, thereby leading to the rolled nanocoils. In this context, a small chemical change in the linker between the 3,5-dimethoxyphenyl group and the PDI backbone will generate a distinct tilting of the polar side chain and thus result in different nanostructures rather than nanocoils.

Indeed, well-defined common nanoribbons were fabricated from compounds **2** and **3** (Figure 1a, which bear linkers with one additional and one less methylene between the 3,5-dimethoxyphenyl group and the PDI backbone, respectively, compared to compound **1**) under identical experimental conditions, as confirmed by TEM (Figures 2d and 2e) and SEM images (Figure S2). These results highlight the essential role of the methylene linker between the 3,5-dimethoxyphenyl group and the PDI backbone that can results in the unique molecular helical stacking arrangement toward the formation of the nanocoil. In addition, the structure of the 3,5-dimethoxyphenyl group is also important for the appropriate tilting and the resultant nanocoil because other polar groups attached to the PDI backbone, even by the methylene linker, did not result in the formation of coiled nanostructures.[7,8,22,23] These observations allow us to conclude that the elaborate design of the polar side chain in asymmetric molecules is essential for the balanced interplay of the non-covalent interactions toward the formation of the coiled nanostructure.

Variations in the molecular orientation within the above nanostructures are also clearly reflected in their optical properties. As shown in Figures 3a and 3b, the absorption and fluorescence spectra of the nanocoils are largely red-shifted compared to that of the individual molecule, indicating the J-aggregate nature of the helical π-stacking geometry within the nanocoil. Compared to the nanocoil from **1**, the nanoribbons from **2** and **3** have considerably less red-shifted absorption and fluorescence spectra (Figure S3), suggesting that the molecules adopt π-stacking with a smaller offset.[8] A prominent feature of the helical π-stacking geometry is the promotion of a transition from the lowest excited state to the ground state, thereby favoring the luminescence property.[2,4] Indeed, a fluorescence quantum yield of 25% (as determined from calibrated integrating sphere measurements) was observed over the nanocoils from **1**, which is considerably higher than those from the nanoribbons from **2** and **3** (11% and 3%, respectively) composed of π-stacks with a smaller offset.

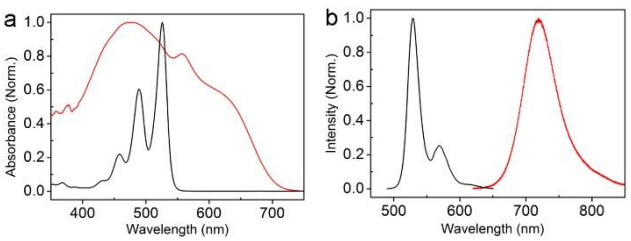

Figure 3 (a) The absorption spectra of the nanocoils from **1** (red) and of isolated **1** in chloroform (black). (b) The fluorescence spectra of the nanocoils from **1** (red) and isolated **1** in chloroform (black).

The efficient emission of the nanocoils, combined with their interior porosity and inherent high surface areas, motivated us to explore their application as a fluorescence sensor. In contrast to the p-type (i.e., electron donating) materials that can be used to sense oxidative reagents such as TNT, the n-type (i.e., electron accepting) PDI nanocoils is suited for sensing reducing reagents like amines. Here, five types of amine vapors (Figure 4c) were selected as the target analytes to evaluate the sensing properties because of their various applications that range from chemical to pharmaceutical to food industries.[6,25,26] In general, when trace phenethylamine vapor (0.3 ppm) was blown onto the nanocoil film formed upon deposition on the Teflon filler film, the fluorescence of the nanocoils was significantly quenched by ca. 18%, as shown in

Figures 4a and 4b. When exposed to other types of amines, prominent fluorescence quenching responses of the nanocoils were also observed (Figure 4c). The fluorescence quenching is due to a photoinduced electron transfer from amines (electron donor) to the excited PDI in the nanocoil (electron acceptor). The large driving force for the photoinduced electron transfer between amines and the excited PDI molecules was previously demonstrated.[6] Considering the uneven film deposition (ranging from 200 to 500 nm), fluorescence quenching measurements were also performed on the film position with different thickness. No distinct variations in quenching efficiency was observed, likely because of the high interior porosity of the nanocoils that facilitates the diffusion of the vapor amines. To determine the detection limit, we also measured the fluorescence quenching efficiency ($1 - I/I_o$) by blowing amine vapor at four different vapor concentrations at room temperature. The quenching data were well fitted by the Langmuir equation, as shown in Figure 4d. Apparently, the fluorescent nanocoils are extremely sensitive to trace amines. Notably, the detection limits of the nanocoils to aniline and phenethylamine were determined to be as low as 0.8 and 3 ppt on the basis of the reliably detectable intensity change of 1%. The higher sensitivity of the nanocoils to aromatic amines over alkyl amines (detection limits of 0.2, 4, and 12 ppb for octylamine, triethylamine, and dibutylamine, respectively) is likely attributed to the stronger binding strength between aromatic amines and the nanocoil via π-π interactions together with the electron donor-acceptor interaction between amines and the nanocoil. Notably, the detection limit of the nanocoils to aniline is 3 orders of magnitude greater than that of previously reported nanofibers.[6] Furthermore, the fluorescence of the nanocoils quenched by amines can be easily recovered through heating at 60 ℃ for 10 minutes, thus enabling them to be used repeatedly (Figure S4). The nanocoil film also demonstrated high selectivity in response to organic amines over other common organic solvents, as shown in Figure 4e. These common organic solvents, even at relatively high vapor concentration, exhibit less than 1 % fluorescence quenching under the same testing conditions. This is because these organic solvent have higher oxidation potential and thereby cannot work as the electron donor to quench the excited PDI in the nanocoil. Interestingly, HCl vapor exhibits sensitive fluorescence quenching (15 % quenching by 25 ppm HCl vapor), as shown in Figure S5. Furthermore, the fluorescence of the nanocoil after exposure to HCl vapor can completely recover in 10 min simply by re-exposing it to air, which is in contrast to the partial recovering after exposure to amines under the same conditions (Figure 4b). This distinct fluorescence recovering behavior can be used to distinguish HCl from amines. The fluorescence quenching by HCl is probably caused by the photoinduced electron transfer between Cl^- and the excited perylene diimide as observed by other group.[27] By contrast, HBr cannot cause the fluorescence quenching because Br^- cannot induce the corresponding photoinduced electron transfer.[27]

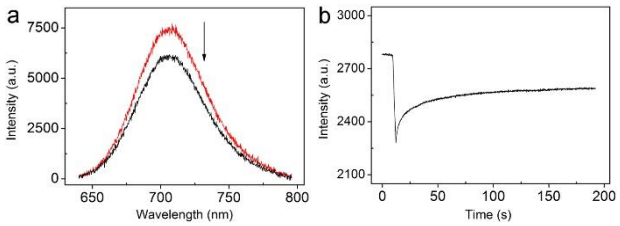

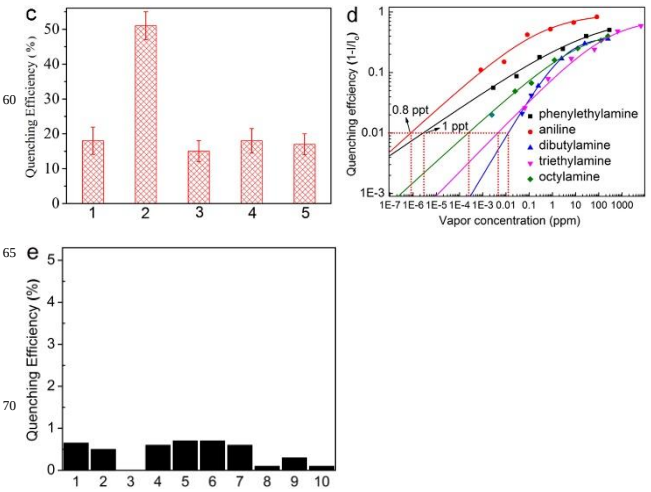

Figure 4 (a) Typical fluorescence spectrum changes of the nanocoils when exposed to 5 mL of blowing phenethylamine vapor (0.3 ppm). (b) Time-course of fluorescence quenching of the nanocoils upon blowing of phenethylamine vapor (0.3 ppm). (c) Columnar comparison of the fluorescence quenching of the nanocoils: 1, phenethylamine (0.3 ppm); 2, aniline (0.8 ppm); 3, octylamine (1 ppm); 4, dibutylamine (2 ppm); 5, triethylamine (7 ppm). (d) Fluorescence quenching efficiency ($1 - I/I_o$) of the nanocoils as a function of the vapor concentration of phenethylamine (data error ±15%). (e) Fluorescence response of the nanocoils to the vapor of common organic solvents: 1, acetone (50 ppm); 2, THF (35 ppm); 3, acetonitrile (25 ppm); 4, chloroform (100 ppm); 5, hexane (60 ppm); 6, cyclohexane (25 ppm); 7, methanol (60 ppm); 8, toluene (16 ppm); 9, acetic acid (20 ppm); 10, nitromethane (30 ppm). All responses have been repeated three times.

Conclusions

In conclusion, we have successfully fabricated thermally stable bilayer nanocoils through elaborate molecular engineering of the polar side chain of an asymmetric PDI molecule. The nanocoil is demonstrated to be highly emissive, with a fluorescence quantum yield of 25%. Upon deposition onto a substrate, such fluorescent bilayer nanocoils with porous interiors exhibited ultrasensitivity to trace amines, with sensitivities that were enhanced by even three orders of magnitude compared to previously reported nanofibers.[6] The design of coiled nanostructures as new sensing materials offers numerous options for optimizing the sensitivities of fluorescence sensors based on organic nanomaterials.

This work was supported by the 973 project (Nos. 2010CB933503, 2013CB632405), NSFC (Nos. 21137004, 2122002, 21377134, 21322701), the "Strategic Priority Research Program" of the Chinese Academy of Sciences (No. XDA09030200), and by the “Youth 1000 Talent Plan” Fund.

Notes and references

[a] *Department of Applied Chemistry, China Agricultural University, Beijing 100193, China. E-mail: jli@cau.edu.cn*
[b] *Key Laboratory of Photochemistry, Institute of Chemistry, Chinese Academy of Sciences, Beijing 100080, China. E-mail: ykche@iccas.ac.cn*

† Electronic Supplementary Information (ESI) available: Details of the synthesis of molecules **1-3** and their self-assembly into their corresponding nanocoils and nanoribbons. The XRD data of the nanocoils, SEM images of the nanorib-bons from 2 and 3, the absorption and fluorescence spectra of aggregates from 2 and 3, and the fluorescence quenching and recovery results. See DOI: 10.1039/b000000x/

‡These authors contributed equally to this work.

1 S. W. Thomas, G. D. Joly and T. M. Swager, *Chem. Rev*., 2007, **107**, 1339.

2 L. Zang, Y. Che and J. S. Moore, *Acc. Chem. Res.*, 2008, **41**, 1596.

3 L. E. Kreno, K. Leong, O. K. Farha, M. Allendorf, R. P. Van Duyne and J. T. Hupp, *Chem. Rev*., 2012, **112**, 1105.

4 C. R. Newman, C. D. Frisbie, D. A. da Silva Filho, J.-L. Bredas, P. C. Ewbank and K. R. Mann, *Chem. Mater*., 2004, **16**, 4436.

5 H. Shao, T. Nguyen, N. C. Romano, D. A. Modarelli and J. R. Parquette, *J. Am. Chem. Soc.*, 2009, **131**, 16374.

6 Y. Che, X. Yang, S. Loser and L. Zang, *Nano Lett*., 2008, **8**, 2219.

7 F. Wurthner, *Chem. Commun*., 2004, 1564.

8 F. Wuerthner, T. E. Kaiser and C. R. Saha-Moeller, *Angew. Chem. Int. Ed.*, 2011, **50**, 3376.

9 T. E. Kaiser, H. Wang, V. Stepanenko and F. Wuerthner, *Angew. Chem.*, **2007**, *119*, 5637–5640; *Angew. Chem. Int. Ed.*, **2007**, 46, 5541.

10 F. J. M. Hoeben, P. Jonkheijm, E. W. Meijer and A. P. J. Schenning, *Chem. Rev.*, 2005, **105**, 1491.

11 M. R. Wasielewski, *Acc. Chem. Res.*, 2009, **42**, 1910.

12 M. C. Ruiz Delgado, E.-G. Kim, D. A. da Silva Filho and J.-L. Bredas, *J. Am. Chem. Soc.*, 2010, **132**, 3375.

13 X.-Q. Li, X. Zhang, S. Ghosh and F. Wuerthner, *Chem. Eur. J*., 2008, **14**, 8074.

14 T. E. Kaiser, V. Stepanenko and F. Wurthner, *J. Am. Chem. Soc.*, 2009, **131**, 6719.

15 Y. Che, D. E. Gross, H. Huang, D. Yang, X. Yang, E. Discekici, Z. Xue, H. Zhao, J. S. Moore and L. Zang, *J. Am. Chem. Soc.*, 2012, **134**, 4978.

16 Y. Che and L. Zang, *Chem. Commun*., 2009, 5106.

17 T. Yamamoto, T. Fukushima, Y. Yamamoto, A. Kosaka, W. Jin, N. Ishii and T. Aida, *J. Am. Chem. Soc*., 2006, **128**, 14337.

18 M. A. J. Gillissen, M. M. E. Koenigs, J. J. H. Spiering, J. A. J. M. Vekemans, A. R. A. Palmans, I. K. Voets and E. W. Meijer, *J. Am. Chem. Soc.*, 2013, **136**, 336.

19 E. T. Pashuck and S. I. Stupp, *J. Am. Chem. Soc.*, 2010, **132**, 8819.

20 L. Chen, K. S. Mali, S. R. Puniredd, M. Baumgarten, K. Parvez, W. Pisula, S. De Feyter and K. Müllen, *J. Am. Chem. Soc.*, 2013, **135**, 13531.

21 W. Zhang, W. Jin, T. Fukushima, N. Ishii and T. Aida, *J. Am. Chem. Soc.*, 2013, **135**, 114.

22 Y. Che, X. Yang, G. Liu, C. Yu, H. Ji, J. Zuo, J. Zhao and Zang, L, *J. Am. Chem. Soc.*, 2010, **132**, 5743.

23 V. Percec, M. Peterca, T. Tadjiev, X. Zeng, G. Ungar, P. Leowanawat, E. Aqad, M. R. Imam, B. M. Rosen, U. Akbey, R. Graf, S. Sekharan, D. Sebastiani, H. W. Spiess, P. A. Heiney and S. D. Hudson, *J. Am. Chem. Soc*., 2011, **133**, 12197.

24 J. Cornil, D. Beljonne, J.-P.Calbert and J.-L. Bredas, *Adv. Mater.*, 2001, **13**, 1053.

25 T. Gao, E. S. Tillman and N. S. Lewis, *Chem. Mater*., 2005, **17**, 2904.

26 J. M. Dragna, G. Pecitelli, L. Tran. V. M. Lynch, E. V. Anslyn and L. Di Bari, *J. Am. Chem. Soc.*, 2012, **134**, 4398.

27 S. Guha, F. S. Goodson, S. Roy, L. J. Corson, C. A. Gravenmier, and S. Saha, J. Am. Chem. Soc., 2011, 133, 15256.